First evidence of widespread, severe soil erosion underneath centre-pivot irrigation systems

Pedro V.G. Batista [a,*], Victor B. da S. Baptista [b], Florian Wilken [a], Kay Seufferheld [a], John N. Quinton [c], Peter Fiener [a]

[a] *Water and Soil Resources Research, Institute of Geography, University of Augsburg, Augsburg, Germany*
[b] *Department of Engineering, Federal University of Lavras, Lavras, Brazil*
[c] *Lancaster Environment Centre, Lancaster University, Lancaster, UK*

* Corresponding author.
E-mail address: pedro.batista@geo.uni-augsburg.de (P.V.G. Batista).

1. Introduction

For at least 5000 years, humankind has been developing irrigated agricultural systems to mitigate droughts and to increase crop production (Gulhati and Smith, 1967). Currently 306 million ha (Mha) of land is under irrigation worldwide, with 240 Mha of this land being converted from rainfed agriculture during the last century (1900–2005) (Siebert et al., 2015). The need for increased agricultural production and to deal with climate change are likely to further increase irrigated areas, alongside with efforts to save water and maximise irrigation efficiency (Puy et al., 2020; Rosa, 2022; Wang et al., 2021).

One approach to improving irrigation efficiency is to adopt centre-pivot irrigation systems. These systems are characterised by a moving lateral line with several emitters, supported above ground by towers that rotate around a central-pivot mechanism, thus irrigating a circular area (Phocaides, 2000). They gained popularity during the second half of the 20th century, arguably due to their high efficiency, application uniformity, and low labour requirements (King, 2016). Currently, centre-pivot irrigation is found in some of the main cereal-producing countries of the world and is the preferred irrigation method in the USA (King, 2016) and Brazil (ANA, 2021). Centre-pivot systems are also being increasingly employed for irrigation in Argentina, China, Portugal, Saudi Arabia, and Spain (Aimar et al., 2022; Johansen et al., 2021; Lian et al., 2022; Silva, 2017).

Centre pivots are often run at low pressure in order to reduce energy demands and decrease operational costs (Baptista et al., 2019). However, lowering the pressure of centre-pivot systems leads to a decrease in sprinkler wetted areas and an increase in droplet sizes, both of which increase water application rates (Gilley, 1984; Hasheminia, 1994). These can be particularly high at the outer spans of large centre pivots, as the discharge per unit length of the lateral line increases proportionally to the distance to the pivot point (Lehrsch et al., 2014).

It follows that peak application rates under the outer span of low-pressure centre-pivot systems can reach 200 mm h^{-1} (King and Bjorneberg, 2011), which exceeds the intensity of most natural rainfall events. Application of water at high intensity leads to infiltration-excess runoff generation, even in highly permeable soils (Hasheminia, 1994; Kincaid, 2002), and it is recognised that runoff and soil erosion can be a significant problem under centre pivots (Kincaid, 2005, 2002; King, 2016; King and Bjorneberg, 2011; Silva, 2006, 2017). Soil erosion in irrigated arable land is particularly problematic because soil degradation resulting from erosional processes can reduce water holding capacity (Batista et al., 2023b) and therefore exacerbate crop vulnerability to droughts (Quinton et al., 2022), which in turn might increase irrigation demands through a positive feedback loop. Despite the recognition that erosion is a problem under centre pivots, research to date has been based on individual field studies where (i) soil and water losses were measured from experimental plots during irrigation (King, 2016; King and Bjorneberg, 2011), and (ii) different management techniques to minimise runoff and soil erosion were tested at the plot scale (Kincaid et al., 1990; Silva, 2017). This means that there is a lack of systematic information regarding the extent and severity of soil erosion in centre-pivot-irrigated land worldwide.

Erosion mapping, where erosion and depositional features are identified from aerial and/or satellite images, offer the best option for assessing the frequency and severity of erosion under centre pivots; and has previously been used in agricultural land over time and across large areas (Fischer et al., 2018; Zweifel et al., 2019). Nevertheless, timing of the images compared to the occurrence of erosion events can be a problem as tillage and crop growth can mask erosion features (Boardman, 2016). Modelling offers an alternative approach and erosion models can be suitable for identifying eroding fields at regional scale, provided that models are fit for purpose and that adequate data is available for parameterisation (Batista et al., 2019). However, to our knowledge there is no model able to reliably simulate soil erosion under centre-pivot systems (see Kincaid, 2002), which ruled out this approach.

Here we investigate the presence and severity of soil erosion underneath centre-pivot irrigation systems using Google Earth™ (GE) imagery. The intensity and frequency of erosion features in 738 centre-pivot fields in the municipality of Cristalina (6154 km^2), state of Goiás, Brazil were mapped. The study area was chosen due to its importance for irrigated cereal production in Brazil and due to the availability of multiple GE images over time. Moreover, the centre-pivot fields in Cristalina represent the cropping systems, soil types, and slope gradients typically found in the Brazilian Cerrado, one of the most important grain-producing regions of the world and the main centre-pivot irrigated zone in Brazil. Importantly, the climate in the region is characterised by a pronouncedly dry winter, which helps to differentiate erosion features associated with either rainfall or irrigation. To the best of our knowledge, this study presents the first systematic, broad assessment of soil erosion severity under centre-pivot irrigation systems.

2. Methods

2.1. Study area

The municipality of Cristalina, state of Goiás, covers an area of 6154 km^2 in the Brazilian Central Highlands (Fig. 1). The region is part of the Cerrado biome, which is characterised by a savannah-like vegetation and a markedly seasonal tropical climate, with rainy summers and dry winters (Aw climate type in Köppen's climatic classification). The average monthly temperature in Cristalina is 21 °C and the average annual precipitation is 1524 mm, which is almost entirely concentrated in the rainy season (September–April) (Alvares et al., 2013) (Fig. 2).

Elevation in Cristalina ranges from 732 to 1255 m a.s.l. (median = 910 m a.s.l.) (Fig. 1). Slopes are mostly gentle (median = 6 %; interquartile range = 3–9 %), coinciding with the occurrence of deeply weathered, leached Ferralsols, on the highest positions of the landscape, and Plinthosols, on hillsides and tableland edges (EMATER, 2016, Marques et al., 2004). Cambisols are found on steeper terrain at the edge of Tertiary erosional surfaces (Marques et al., 2004). The eastern area of the municipality is drained by the São Marcos River, whilst the western area is drained by the Corumbá River, both of which are part of the Paraná basin.

Land use in Cristalina is characterised by an intensive agriculture, which expanded into the Brazilian Cerrado in the second half of the 20th century. This resulted in the conversion of low fertility soils to crop production by liming and high fertiliser input (Lopes and Guilherme, 2016). Currently, the Cerrado region is one of most important grain-producing areas in the world and arguably Brazil's most threatened biome (Garrett et al., 2018; Hunke et al., 2015). In Cristalina, permanent and annual cropland occupy about 34 % of the municipality area (IBGE, 2017). As in most of the Cerrado, the main harvested crops are soyabeans (*Glycine* max), maize (*Zea mays*), and common beans (*Phaseolus vulgaris*) (IBGE, 2017). Importantly, Cristalina is in the main centre-pivot irrigation zone of Brazil and is the municipality with the third largest centre-pivot irrigated area in the country, with 783 pivots that irrigate an area of approximately 60,000 ha (mean irrigated area per centre pivot is 76 ha) (ANA, 2021).

Year-round use of centre-pivot systems means that soils are not only exposed to erosive water drops in the rainy season, but throughout the year. Centre-pivot irrigation in Cristalina (and throughout the Brazilian Cerrado) allows for 4–5 crops for every two crop years, with a typical crop rotation of soyabeans (1st crop, sowed in Sep/Oct) followed by maize (2nd crop, sowed in Jan/Feb/Mar), potentially followed by common beans (3rd crop, sowed in Apr/May) (ANA, 2021). Irrigation is used to supplement water deficits for the 1st crop in the case of dry spells during summer; to increase productivity for the 2nd crop, which is partially grown during the dry season; and to irrigate the third crop, which relies almost entirely on irrigation water (ANA, 2021).

2.2. Classification of erosion features

To assess the severity and extent of soil erosion underneath centre pivots in Cristalina, we examined satellite images available from Google Earth™ (GE). These images are free to access and allow for the identification

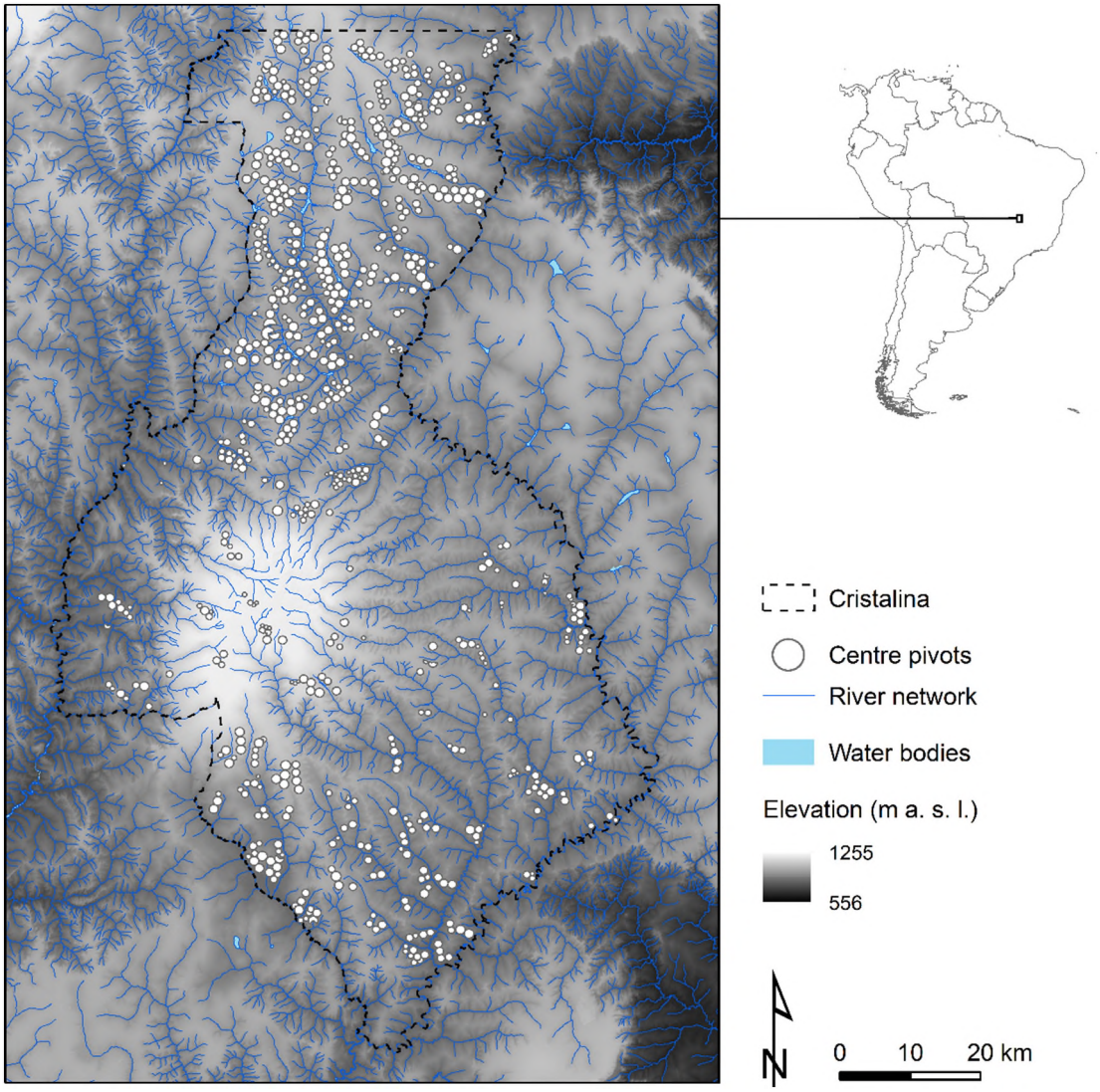

Fig. 1. Digital elevation model (DEM), hydrography, and centre-pivot-irrigated fields in the municipality of Cristalina, Brazil. Circle sizes represent the area of the centre-pivot fields, which range from 9 to 172 ha (mean = 76 ha).

of erosion features, such as rills and ephemeral gullies, with comparable results to field-mapped data (Boardman, 2016). The location of each centre pivot in the study area was taken from the Brazilian Irrigation Atlas (ANA, 2021), which used multiple satellite images to identify centre-pivot fields in Brazil for the year of 2019.

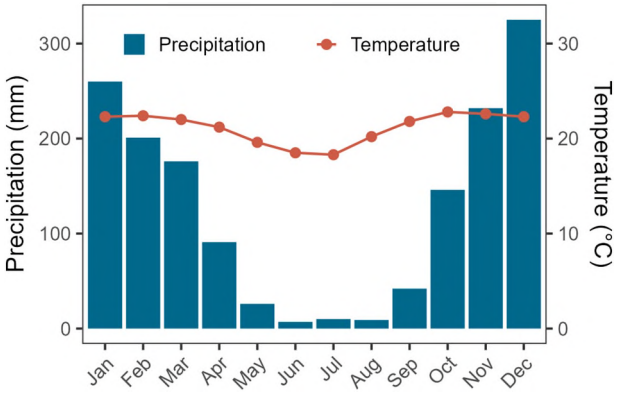

Fig. 2. Long-term average monthly temperature and rainfall (1950–1990) for the municipality of Cristalina, Brazil. Data from Alvares et al. (2013).

Our approach consisted of ranking erosion severity classes based on a visual interpretation of erosion features (Fischer et al., 2018). Since the timing of GE images is somewhat arbitrary and spatially heterogeneous, we decided to analyse the last five images available for the location of each centre-pivot field. Hence, the image dates and the number of available images may vary between individual fields. To reduce the potential for misclassifications, we did not consider depositional features, interrill erosion, or signs of soil truncation. Instead, we focused on identifying linear erosion features, which are more easily distinguishable in the images. For simplicity, hereon these linear features will be referred as erosion rills, although some might be considered ephemeral gullies.

As such, we predefined four erosion classes:

- Class 0: no visible erosion rills underneath the centre-pivot area (Fig. 3a).
- Class 1: legacy rills still visible after tillage, harvest, or crop growth; not actively eroding at the time of the image (Fig. 3b).
- Class 2: visible, active rills with a maximum length shorter than ¼ of the pivot diameter; rill-affected area <25 % of the field area (Fig. 3c).
- Class 3: visible, active rills with a maximum length longer than ¼ of the pivot diameter; or rill-affected area >25 % of the field area (Fig. 3d).

In August 2022, one classifier (Classifier #1, trained researcher in soil erosion) performed an initial classification of all centre-pivot fields, using

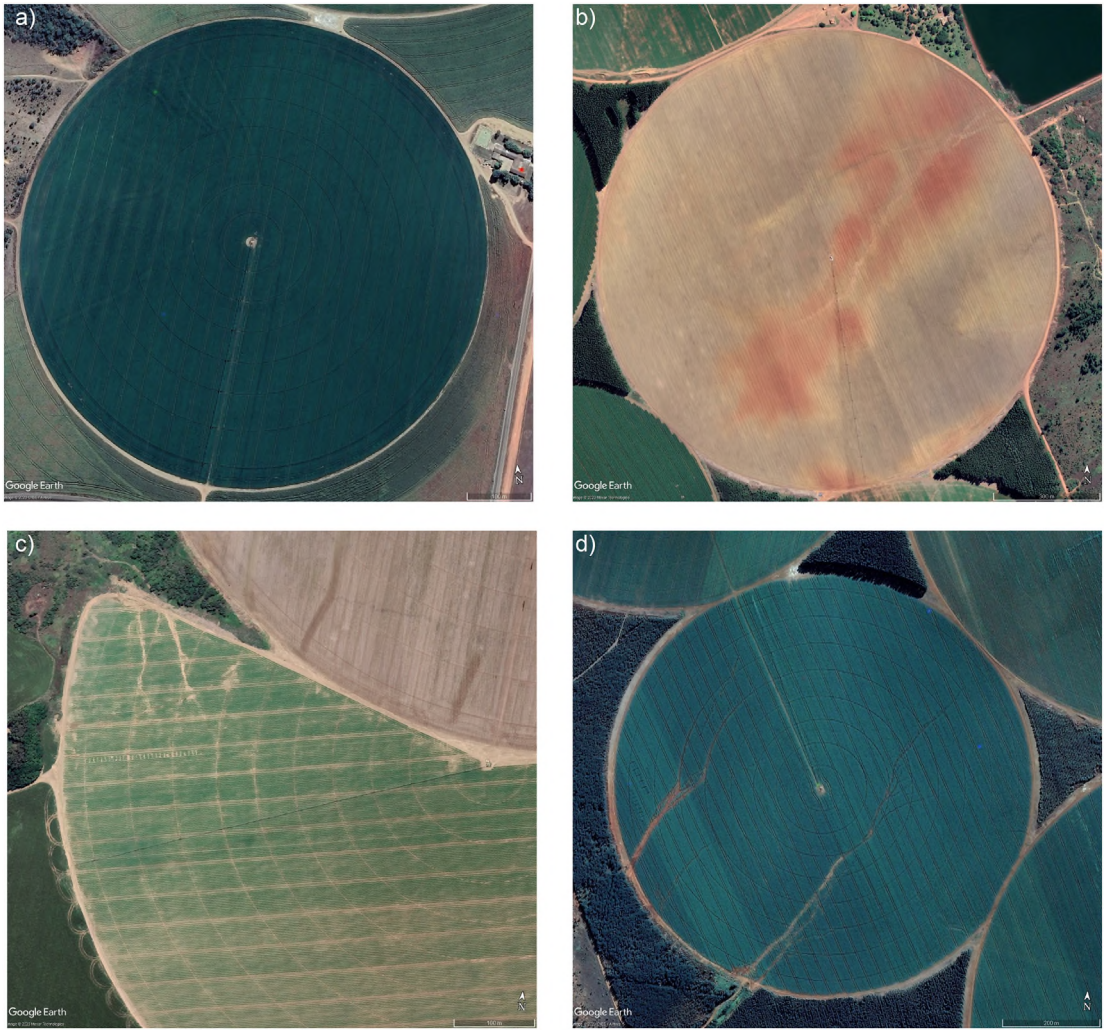

Fig. 3. Classification example: a) Centre-pivot field (Jun 2021) with no signs of rill erosion (Class 0); b) Centre-pivot field (May 2020) with legacy signs of rill erosion (Class 1); c) Centre-pivot field (May 2019) with longest rill < ¼ of the pivot diameter (Class 2); d) Centre-pivot image (July 2019) with longest rill > ¼ of the pivot diameter (Class 3). Imagery from Google Earth™.

the latest available images in GE, as described above. This same classifier then reanalysed all the centre-pivot-field images with the presence of erosion features (Classes >0), this time measuring the length of the longest rill per centre-pivot image and correcting for false positives. From October to December 2022, two additional classifiers (Classifier #2 and Classifier #3, trained researchers in soil erosion) accomplished another classification of all centre-pivot fields (25 % of the pivots by Classifier #2, 75 % of the pivots by Classifier #3). This was performed to evaluate the agreement between the classifiers and to provide an assessment of classification error, which was quantified by a confusion matrix, Cohen's kappa coefficient, and the root mean square deviation (RSMD) of the categorisations (Classes 0 to 3). The kappa coefficient ranges from −1 to 1, with values close to zero indicating the majority of the agreement may be random and values above 0.4 indicating a satisfactory agreement, while below −0.4 indicating a systematic disagreement. The RMSD takes the same unit as the target variable and ranges from 0 to infinity, with lower values indicating a higher agreement between the classifications (see Bennett et al., 2013 for formulae and interpretation of the metrics). Of note is that the additional classifiers were also responsible for identifying the presence of soil conservation structures (e.g., broad-based terraces and grassed waterways), offsite pollution-control structures (e.g., along-road and in-field retention basins), and potential triggers for rill incision (e.g., compacted tramlines, Saggau et al., 2022, Silgram et al., 2010) in the centre-pivot fields. Moreover, to interpret the classification outputs we used terrain attributes (slope gradient and flow distance to the nearest stream channel) derived from a 30 m × 30 m resolution digital elevation model (DEM) from the Shuttle Radar Topography Mission (SRTM) and the areas of the centre-pivot fields available from the Brazilian Irrigation Atlas (ANA, 2021). The differences in terrain attributes and field sizes between eroding and non-eroding pivots was evaluated with the Kruskal-Wallis H test and all statistical/data analyses were performed in R (R Core Team, 2023).

3. Results and discussion

3.1. Classification of erosion features in centre-pivot fields and its accuracy assessment

We classified 738 from the 783 centre-pivot fields mapped in Cristalina by the Brazilian Irrigation Atlas (ANA, 2021) (total area = 56,462 ha). The remaining fields (45) could not be identified by at least one of the classifiers during the image analysis, e.g., the pivots were not present when the GE images were taken.

Approximately four images per centre-pivot field were analysed. Thus, a total of 2950 centre-pivot-field images were analysed by Classifier #1 and 2966 by Classifiers #2 and #3, combined. The slightly larger number of centre-pivot-field images analysed by the Classifiers #2 and #3 was explained by the availability of more recent GE images when they performed their classification, which led to a difference in the dates of the images

analysed by the classifiers. For instance, Classifiers #2 and #3 analysed 62 centre-pivot-field images from 2022, while only one field-image from this year was evaluated by Classifier #1. Accordingly, the median period covered by the GE images per centre-pivot field was three years, for Classifier #1, and four years for Classifiers #2 and #3. In both cases the median year of the images per centre-pivot field was 2019.

To estimate the agreement between classifiers, 2188 centre-pivot-field images were classified twice. Classifiers #2 and #3 identified signs of erosion in 331 centre-pivot fields (Class >0 for at least one of the available GE images). Classifier #1 was more conservative identifying 238 eroding fields, possibly due to the additional classification performed during the measurement of rill lengths (see Section 2.2). The identification of centre-pivot fields with the presence of erosion features had an overall agreement between classifiers of 80 % (76 % for non-eroding fields and 87 % for eroding fields) (Cohen's kappa = 0.59). The differences between the classifiers stemmed from missing small signs of rill erosion, mistaking cattle trails for rills, and potential typing errors when tabulating the data. The longer period covered by the GE images per centre-pivot field available for Classifiers #2 and #3 might have also increased their identification of centre-pivot-field images with erosion features.

According to the matching classifications, 211 centre-pivot fields displayed signs of rill erosion, which corresponded to 29 % of 738 analysed fields (Fig. 4). The eroding centre-pivot fields were more likely to be identified when a larger number of images from different timepoints were available (Fig. 5). This highlights the importance of the timing of the image corresponding with the period of erosion events when identifying erosion features (Boardman, 2016; Fischer et al., 2018). It also points out that our approach underestimates the number of eroding fields for the areas with fewer images.

If we considered only the 2188 centre-pivot-field images with matching image dates, it was clear that the disagreements between classifiers were mostly associated to the assignment of neighbouring categories (Cohen's kappa = 0.53; RMSD = 0.24) (Fig. 6). This pattern was particularly evident for erosion classes 1 and 2, which displayed the lowest classification agreement (74 % and 72 %, respectively). The discrepancies in these classes were expected, as the identification of smaller rills is error prone. Moreover, distinguishing what constitutes a legacy rill, compared to an actively eroding one, is partially subjective. Nevertheless, Classifier #1 assigned a greater proportion of eroding centre-pivot images to Class 3 (29 %) and a lesser proportion to Classes 1 and 2 (38 % and 33 %, respectively), compared to Classifiers #2 and #3 (Class 1 = 44 %, Class 2 = 37 %, Class 3 = 19 %) (Fig. 6).

To increase the confidence in our soil erosion assessment, we focused the remainder of our results and discussion on the centre-pivot fields and centre-pivot-field images where classifications agreed. A shapefile containing the location of the centre-pivot fields, their erosion classification, and the date of the analysed GE images has been uploaded to an open-access data repository (Batista et al., 2023a). Moreover, in the following sections we provide a centre pivot identification number (Pivot ID) for all figures which display GE images of centre-pivot fields. This number is taken from the Brazilian Irrigation Atlas (ANA, 2021) and can be used to identify the centre-pivot fields in the above-mentioned shapefile.

3.2. Temporal patterns of soil erosion in centre-pivot irrigated fields

Most erosion features were identified during the dry season of the Brazilian Cerrado, using images from May, June, and July (Fig. 7). This was related to the greater availability of GE images with low cloud cover during this period of the year. Erosion features were identified in more than one image for 52 % of the eroding centre-pivot fields. This frequent identification of active, severe signs of rill erosion during periods with very low rainfall indicates that centre-pivot irrigation might be either aggravating or initiating soil erosion. As argued by Boardman and Evans (2020), the timing of erosion monitoring is critical, as erosion signs are easily be masked by vegetation – particularly in the humid tropics.

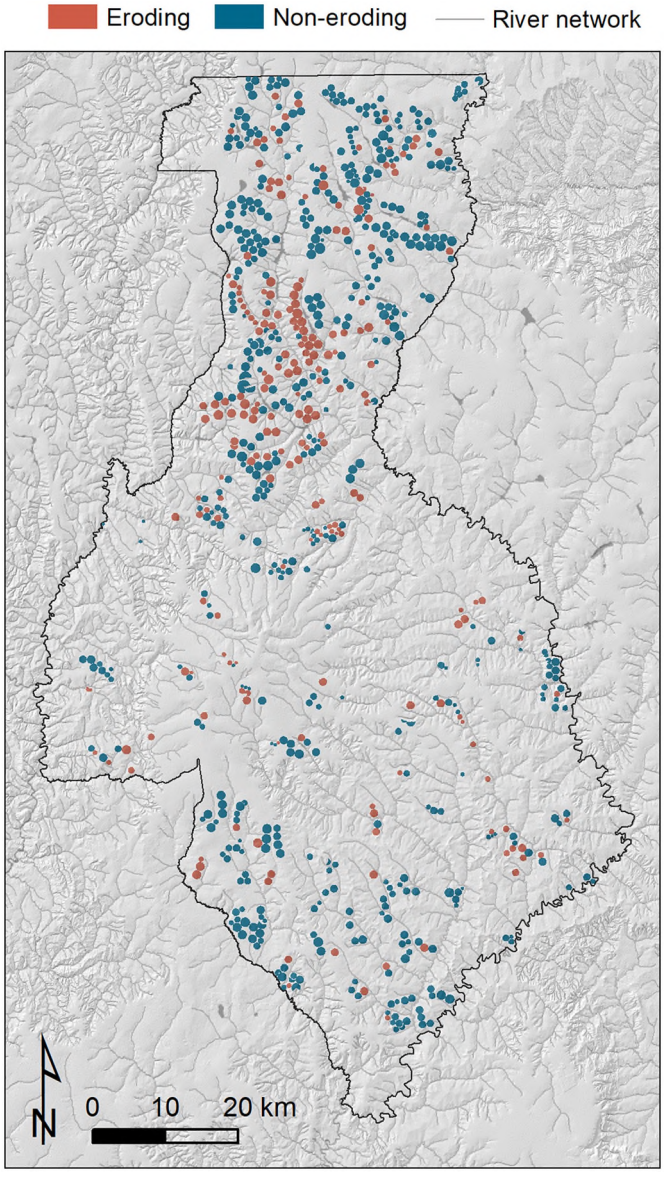

Fig. 4. Location of eroding and non-eroding centre-pivot fields in Cristalina, Brazil. Only those fields where both classifiers identified erosion features were considered to be eroding. Circle sizes represent the area of the centre-pivot fields, which range from 9 to 172 ha (mean = 76 ha).

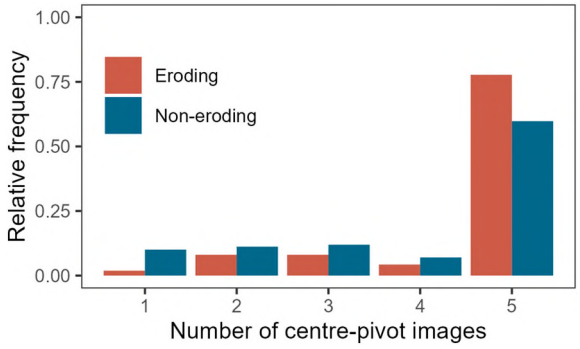

Fig. 5. Relative frequency (0–1) of the number of GE images per centre-pivot field for eroding and non-eroding fields.

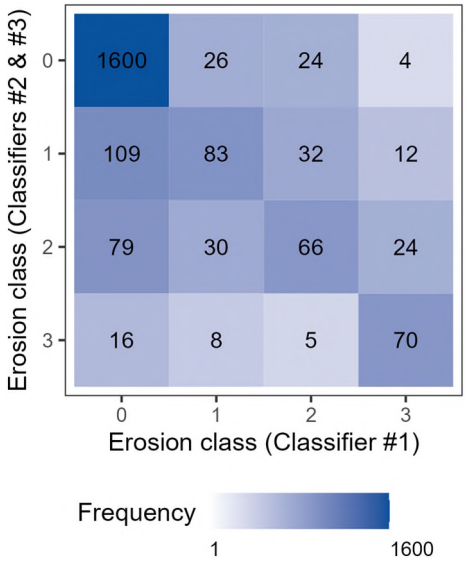

Fig. 6. Confusion matrix for the erosion-feature classes assigned by Classifier #1 and Classifiers #2 and #3 for the centre-pivot-field images. Each column represents the classes assigned by Classifier #1. The rows represent the classes assigned by Classifiers #2 and #3. Numbers in the boxes refer to the frequency of erosion classes assigned by the classifiers.

As rills incised during the rainy season would have been at least partially filled up during tillage, harvesting, and sowing of the subsequent crops (Fig. 8a), the erosion features identified in the months of May to July are likely to be associated with the second or third crop in the rotation. Active erosion features (Classes 2 and 3) associated with the third crop (typical sowing dates from April to May), provide evidence that irrigation is the driver of soil erosion underneath the centre-pivots (Fig. 8b). In cases where active rills were found in the second crop, we cannot disregard the hypothesis that the channels were already established by rainfall erosion at the end of the rainy season, which coincides with the sowing dates (Fig. 7) and the early development stages of the second crop. Erosion can also be linked to climatic anomalies leading to rare erosive rainfall events in the beginning of the dry season, e.g., above-average rainfall was reported within the study area in April and May 2019. However, the severity, extent, and persistence of the soil erosion features identified during the height of the dry season indicate that, at the very least, irrigation is partially responsible for the activity of rills (Fig. 8d). There is also evidence that centre-pivot irrigation promoted soil erosion in previously established rill channels (Fig. 8c).

The occurrence of erosion under centre pivots can be attributed to the water application rates, which typically reach 60 to 200 mm hr^{-1} (King and Bjorneberg, 2011). Such application rates are likely to exceed many of the soil infiltration capacities in the region (around 50 mm hr^{-1} for Ferralsols in the Cerrado, Panachuki et al., 2011) and may initiate overland flow and soil erosion. Moreover, rill incision can be triggered due to the breaching of compacted centre-pivot wheel tracks (for example, Fig. 8b,d).

3.3. Extent and drivers of soil erosion in centre-pivot-irrigated fields

The median length of the longest rill per centre-pivot image was 260 m (interquartile range = 151–440 m), with a maximum value over 1200 m (Fig. 9). These rill lengths are some of the longest described in the scientific literature and exceed those found in Boardman (2016), Fischer et al. (2018), Prasuhn (2020), and Van Oost et al. (2005). Rills underneath centre pivots in Cristalina appear commensurate to gully networks, such as those developed in olive orchards in Spain (Castillo et al., 2012). In some cases, the centre-pivot images illustrate widespread signs of soil erosion over a large proportion of the field, significantly impacting on crop production (Fig. 10).

The large field sizes found under the centre pivots is likely to be responsible for the length of the Cristalina rills exceeding those of Central Europe and the UK, where field sizes are much smaller and land use is much patchier. For example, a single centre pivot in Cristalina can cover an area larger than the 94 ha experimental catchment where Cerdan et al. (2002) monitored rill erosion in multiple fields with areas of 1–10 ha.

The analysed images also indicate off-site erosion impacts. Runoff from the centre pivots flows downslope into adjacent fields, even during the dry season (Fig. 11a). Moreover, the concentrated flow from within the centre-pivot irrigated areas sometimes crosses adjacent roads and field boundaries, creating rill channels across downslope fields (Fig. 11b). Additionally, we observed soil erosion off-site effects associated to the runoff connectivity to surface waters (Fig. 11c,d). Since runoff from agricultural land is often linked to the transport of particulate and dissolved pollutants (Didoné et al.,

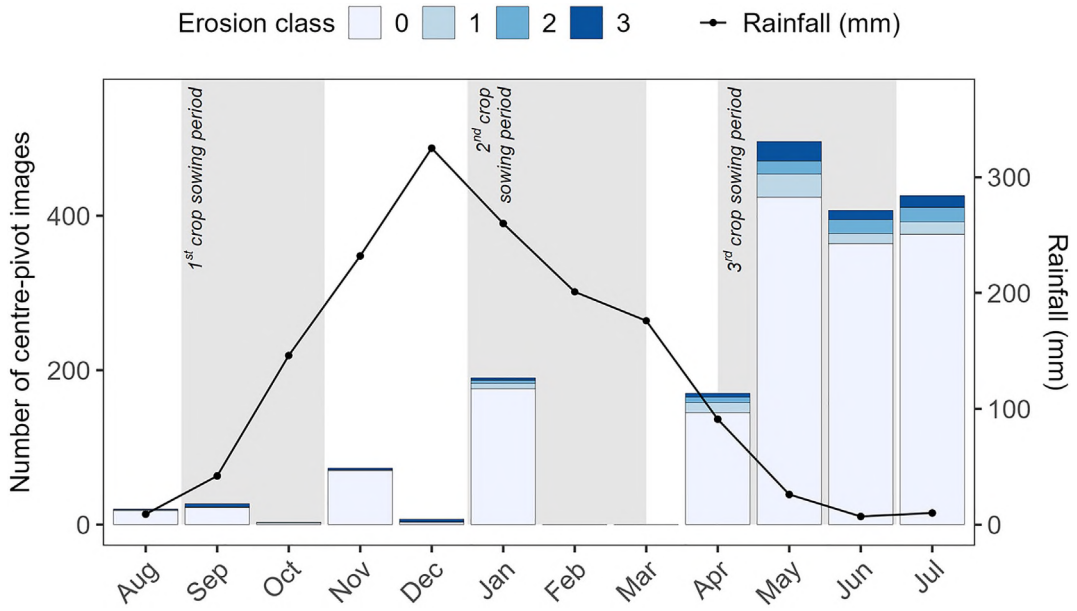

Fig. 7. Number of analysed centre-pivot fields according to the month of the year of the GE images. Rainfall data from Alvares et al. (2013).

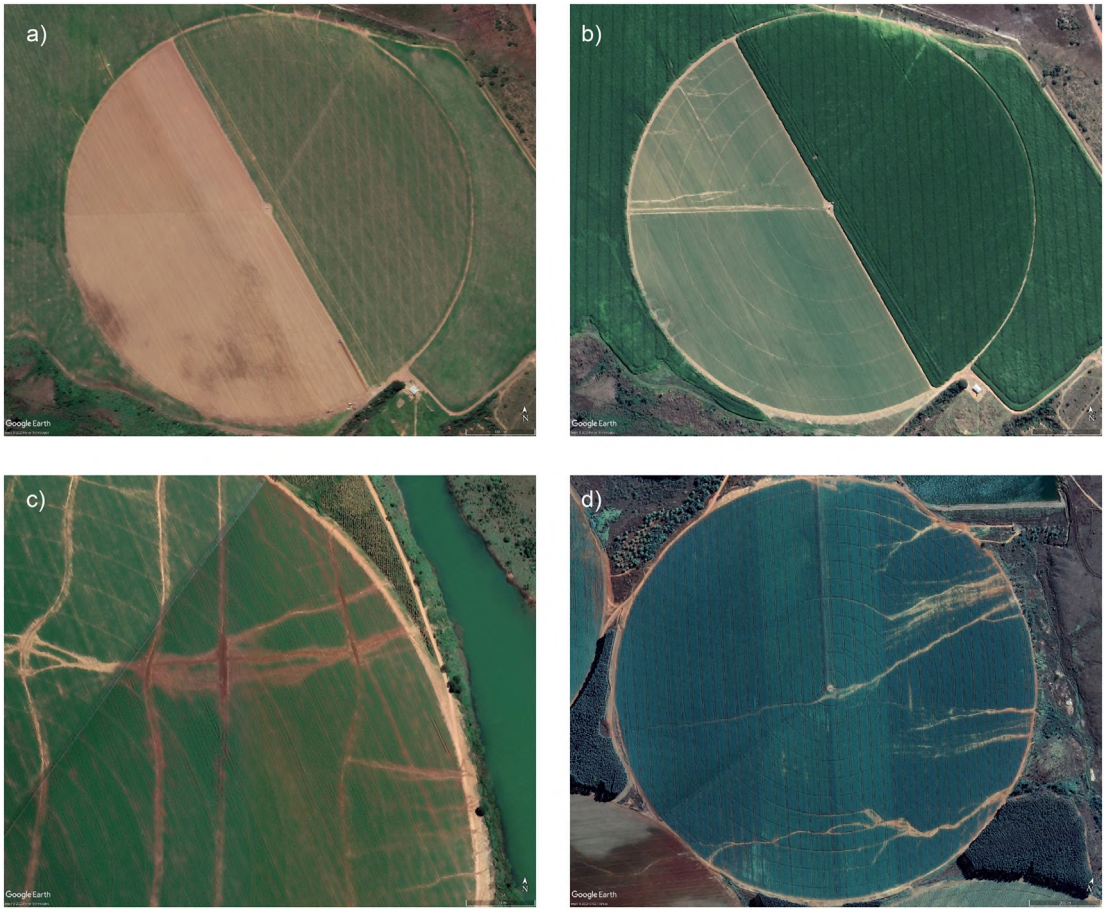

Fig. 8. a) Freshly tilled soil in a centre-pivot field in April 2020 (Pivot ID 17149, diameter = 620 m). b) Soil erosion for the same field (Pivot ID 17149) in May 2020: rills initiated from the centre-pivot circular wheel tracks, as seen on the top-left centre-pivot quadrant, and from a linear feature leading to the pivot. c) Soil erosion during centre-pivot irrigation in April 2018: darker-red (wet) soil can be seen moving along the rills and being deposited on adjacent dirt roads while the irrigation tower moves counter clockwise (Pivot ID 16629, diameter = 1370 m). d) Extensive rill network across the centre-pivot-field diameter in July 2019 (Pivot ID 11705, diameter = 1115 m); breached circular centre-pivot-wheel tracks lead to rill incision, parallel tracks supply sediment and runoff to the incised rill network. Imagery from Google Earth™.

2021; Quinton and Catt, 2007), the overland flow originating from underneath centre pivots and moving into surface waters poses a threat to water quality and supply in Cristalina.

Regarding the causes of soil erosion in the centre-pivot-irrigated fields, we found that rill incision was often linked to centre-pivot-wheel tracks (e.g., Figs. 11c, 8b,d), which were identified as the direct cause for rill development in at least 51 centre-pivot-field images. These tracks can undergo severe compaction if the lateral tower is moving over ponded or saturated soil, creating deep circular channels that intercept runoff within the irrigated fields (Kincaid, 2002) (Fig. 12). We identified that rill incision occurred as these circular channels collected runoff and sediment along the flow path, until reaching a point in which the topographical flow direction becomes roughly perpendicular to the tangent of circular wheel track. At this stage, the concentrated flow breaks through the compacted wheel-channel banks (Fig. 11c). The rill may also cross parallel tracks, where it might receive runoff and sediment from that track, creating a highly connected rill network (Fig. 8d).

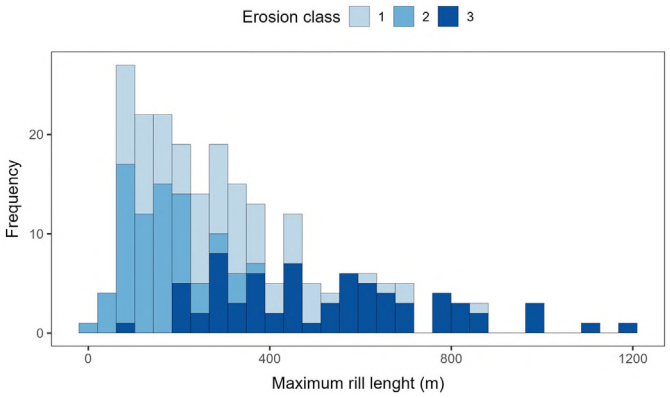

Fig. 9. Stacked histogram of the longest rill lengths per centre-pivot field observed in the GE images for irrigated areas in Cristalina, Brazil.

The DEM-extracted terrain attributes from the centre-pivot fields further allow us to draw conclusions about the locations of the eroding centre pivots: (i) eroding centre-pivot fields were located in areas with significantly higher slopes ($p < 0.01$) than the fields without erosion features (median slope for eroding fields = 4.7 %, median for non-eroding fields = 3.8 %, Fig. 13); (ii) the eroding fields had significant shorter distances along the flow path to the nearest stream channels ($p < 0.01$) (median = 263 m, Fig. 13) compared to the non-eroding (median = 452 m, Fig. 13), indicating the incision of erosion rills in flow-accumulating, concave positions of the landscape. There was no significant difference between eroding and non-eroding centre-pivot-field sizes ($p = 0.60$).

The main soil conservation and offsite pollution control structures currently employed in the centre-pivot fields were retention basins and broad-based terraces (Fig. 14). Of note is that soil conservation practices, particularly terracing, were more frequently identified in the eroding

Fig. 10. Severe signs of soil erosion over a large proportion of the centre-pivot field (Pivot ID 11508, diameter = 800 m), compromising crop yields in the affected area (about 30 % of the field) (May 2020). Adjacent rainfed, terraced cropland on the right side of the image does not show similar erosional features. Imagery from Google Earth™.

centre-pivot fields, compared to the non-eroding (Fig. 14). This is possibly the result of terraces being established as a means to counteract soil erosion, rather than preventing it. However, improvised terraces (i.e., not properly designed along contour lines), seemed to be ineffective in stopping soil erosion once rill channels were already incised (Fig. 8c).

3.4. Perspectives for managing soil erosion in centre-pivot-irrigated fields in the Brazilian Cerrado

The extent and severity of soil erosion features under centre-pivot irrigation systems in Cristalina are leading to significant land degradation. Based on the analysis of potential causes of soil erosion in the area, we can recommend a number of management practices to control soil erosion and surface runoff in centre-pivot-irrigated fields in the Brazilian Cerrado.

To address management challenges associated with centre-pivot irrigation, such as high water-application rates and the potential for wheel-track compaction, soil conservation practices that promote soil cover and soil-water infiltration and prevent harmful runoff concentration during both irrigation and the summer-concentrated rainfall are required. These include zero tillage, reservoir tillage, broad-based terracing, retention basins, and grassed waterways (Fiener and Auerswald, 2003; Hörbe et al., 2021; Silva, 2017). Although zero-tillage is widely employed in the Brazilian Cerrado, this technique alone is not always sufficient to prevent soil erosion and combining it with other soil conservation practices, such as broad-based terracing, has been shown to be more effective (e.g., Didoné et al., 2017; Londero et al., 2021).

Adequate design and operation of centre-pivot systems are as important as soil management for preventing runoff and erosion during irrigation (Lehrsch et al., 2014). If properly managed, centre-pivot systems can be highly effective and have been shown to improve soil and surface water quality in areas where furrow irrigation was used previously (Bjorneberg et al., 2020; Ippolito et al., 2017). Appropriate management entails applying an optimum water depth and at the right time (based on crop demands, at smaller depths with higher frequency), at intensities that allow for soil-water infiltration. To this end, booms (or offset booms or boom backs) on alternate sides of the centre-pivot lateral line are an effective approach for reducing water application rates by increasing the sprinkler wetted area (Nakawuka et al., 2014). Moreover, boom backs designed to extend the sprinklers behind centre-pivot wheels can keep wheel tracks dry until the lateral passage, which reduces the potential for tyre-rut formation (Martin et al., 2017). This is critical, as our results indicate that avoiding soil compaction on the centre-pivot-wheel tracks should be a priority. Variable-rate sprinklers can also help preventing runoff by use of a variable discharge rate depending on field characteristics (Martin et al., 2017). On top of management practices, it is important to highlight that the design of centre pivots can be improved to minimise the risk of overland flow and soil erosion by (i) avoiding long lateral lines with excessive discharge at their outer spans, and (ii) choosing appropriate wheels/tyres to avoid soil compaction.

Ultimately, controlling soil erosion and surface runoff in centre-pivot-irrigated fields in the Brazilian Cerrado is crucial to avoid the erosional effects that exacerbate crop vulnerability to droughts (Quinton et al., 2022). For instance, soil erosion by water selectively removes finer soil particles and soil organic carbon, reducing soil water holding capacity and increasing runoff propensity (Batista et al., 2023b). Hence, erosion is likely to increase irrigation demands, as a lesser proportion of the precipitation becomes eventually available to plants, creating a highly undesirable positive feedback loop between irrigation and soil erosion.

4. Conclusions

Here we have used Google Earth™ (GE) images to map erosion features for 738 centre-pivot fields (total area = 56,462 ha) in the municipality of Cristalina, in the Brazilian Cerrado. We found that:

i) at least 29 % of centre-pivot fields in the study area displayed signs of rill erosion over the latest five available GE images at the time of the analysis (median image year per centre-pivot = 2019, median image range per centre-pivot = 3 years),
ii) rills were mostly identified during the dry season, which coincided with time of the year of greater image availability, and
iii) the median length of the longest rill per centre-pivot field was 260 m, with maximum values over 1200 m.

The consistent identification of widespread, severe erosion features underneath the centre-pivots during the dry season of the Brazilian Cerrado strongly suggests that irrigation causes or aggravates erosion in the study area. Our analysis further demonstrated how centre-pivot irrigation can directly cause soil erosion, due to excessive application rates in periods of very low rainfall; or indirectly, due to the creation of circular pivot-wheel-track channels that are breached in flow-accumulating concavities and promote rill incision. Furthermore, we found that eroding centre-

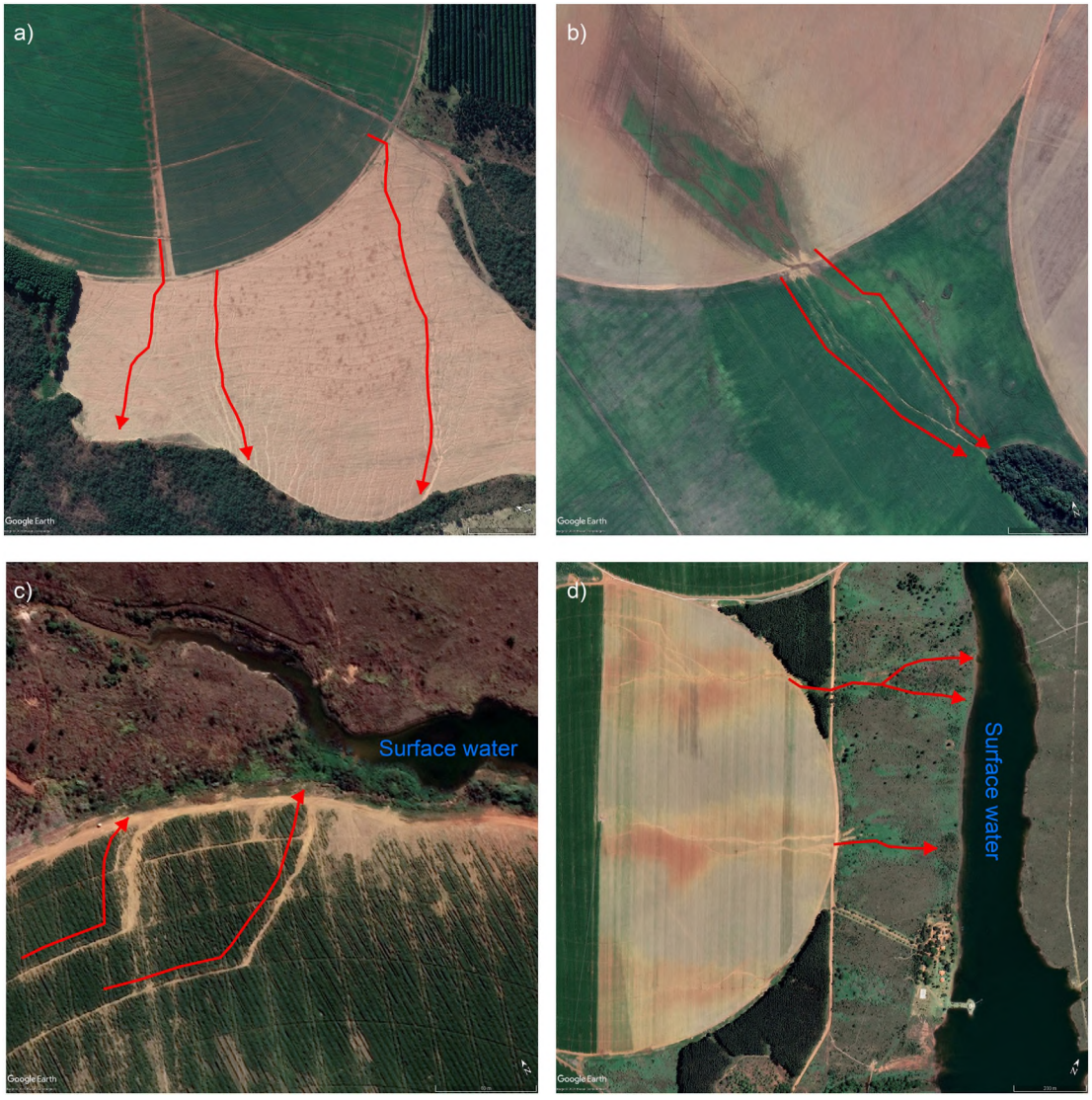

Fig. 11. a) Extensive erosion in a fallow field downslope from a centre pivot (Pivot ID 12214, diameter = 930 m) during the dry season (July 2018): rills initiate along the flow paths from the irrigated upslope field. b) Erosion rills starting from the outflow of a grassed waterway of a centre-pivot field (Pivot ID 11816, diameter = 1100 m) and cutting through a downslope rainfed field until reaching a woodland (May 2020). c) Eroding centre-pivot field (Pivot ID 11697, diameter = 1230 m) close to surface water: rills initiate from breached centre-pivot-wheel tracks and flow downslope towards the stream network (June 2021). d) Runoff path downstream from an eroding centre-pivot field (Pivot ID 11685, diameter = 1240 m) connecting with surface water (April 2018). Imagery from Google Earth™.

pivot fields in Cristalina were more likely to be found in the proximity of surface waters, which increases the risk of sediment and pollutant delivery to water courses.

To the best of our knowledge, this is the first systematic report of widespread and severe soil erosion under centre-pivot-irrigated fields worldwide. As centre pivots are already the preferred irrigation method for many important crop-growing regions in the world and their use currently expanding to many other areas, our contribution raises a timely concern about the sustainability of centre-pivot irrigation systems. However, the risk of runoff and soil erosion can be attenuated by management practices (e.g., avoiding centre-pivot-wheel track compaction, adopting combined soil-conservation practices) and improved pivot design (e.g., reducing pivot sizes).

Although the potential for soil erosion underneath centre pivots has been recognised for some time, our results demonstrate how this can indeed be a serious, systematic issue in areas without appropriate soil and irrigation management. Hence, it is crucial to further develop technologies that allow for the assessment of irrigation-induced soil erosion across large areas. As such, adapting soil erosion models and developing machine learning approaches for automated feature identification might assist in the detection and quantification of erosion under centre-pivot irrigation systems, as they expand worldwide.

CRediT authorship contribution statement

PVGB: Conceptualisation, Methodology, Formal analysis, Investigation, Visualisation, Writing – Original Draft Preparation. VBSB: Conceptualisation, Investigation. FW: Methodology, Investigation, Writing – Reviewing and Editing. KS: Methodology, Investigation. JNQ: Writing – Reviewing and Editing, Supervision. PF: Writing – Reviewing and Editing, Supervision.

Data availability

The Google Earth™ images used in this research are free to access and available from Google Earth Pro on Desktop (https://www.google.com/earth/versions/#earth-pro). The digital elevation model used for the terrain

Fig. 12. A centre-pivot wheel creating a compacted track as it moves over wet soil with surface ponding in Macaia, Minas Gerais, Brazil. Photo from Victor B. S. Baptista.

analysis can be downloaded freely from the USGS Earth Explorer (https://earthexplorer.usgs.gov/). The centre-pivot shapefile from the Brazilian Irrigation Atlas is available at: https://metadados.snirh.gov.br/geonetwork/srv/api/records/e2d38e3f-5e62-41ad-87ab-990490841073. The results from the erosion classification per centre-pivot field were uploaded to a data repository and are available at: doi:https://doi.org/10.5281/zenodo.7680625 (Batista et al., 2023a).

Declaration of competing interest

The authors declare no competing interests.

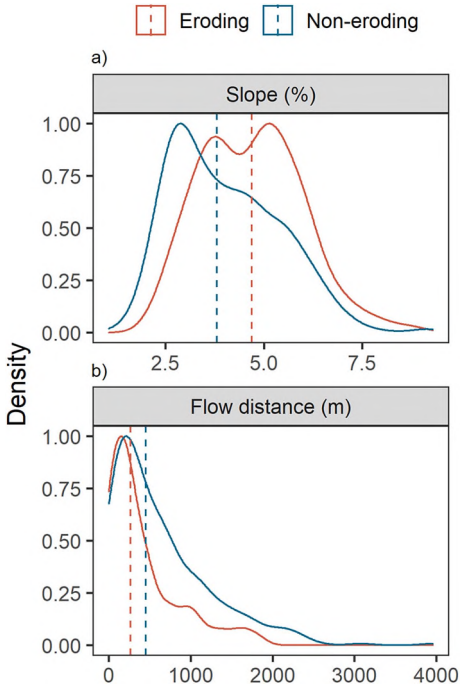

Fig. 13. Scaled probability density function of the mean slope (%) per centre-pivot field (a) and minimum flow distance to the nearest stream channel (m) per centre-pivot field (b) in Cristalina, Brazil. Dashed lines represent group medians (eroding, non-eroding).

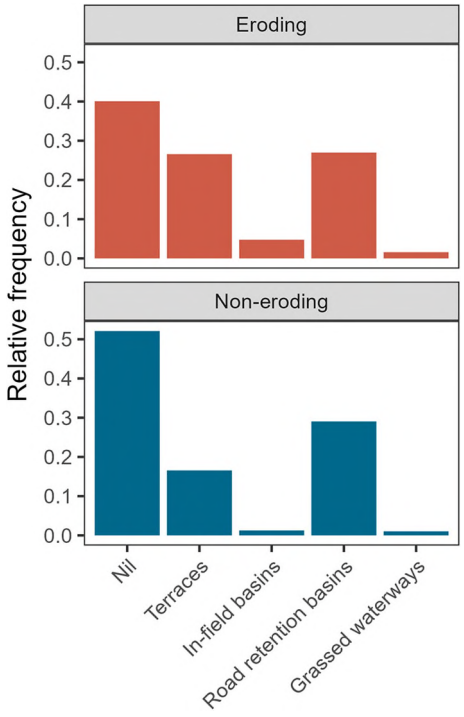

Fig. 14. Relative frequency (0 – 1) of soil conservation and offsite pollution-control structures observed in centre-pivot fields in Cristalina, Brazil.

Acknowledgements

We acknowledge the use of Google Earth™ imagery ©2023 Google for Figs. 3, 8, 10, and 11. Pedro V G Batista was supported by German Federal Ministry of Food and Agriculture (Grant No. 28DK118B20). The cooperation between Brazilian and Bavarian research institutions was supported by the Bavarian Academic Centre for Latin America (BAYLAT).

References

Aimar, F., Martínez-Romero, Á., Salinas, A., Giubergia, J.P., Severina, I., Marano, R.P., 2022. A revised equation of water application efficiency in a center pivot system used in crop rotation in no tillage. Agronomy 12, 2842. https://doi.org/10.3390/agronomy12112842.

Alvares, C.A., Stape, J.L., Sentelhas, P.C., De Moraes Gonçalves, J.L., Sparovek, G., 2013. Köppen's climate classification map for Brazil. Meteorol. Z. 22, 711–728. https://doi.org/10.1127/0941-2948/2013/0507.

ANA – Agência Nacional de Águas e Saneamento Básico, 2021. Atlas Irrigação. Uso da água na agricultura irrigada. 2nd ed. Agência Nacional de Águas e Saneamento Básico. ANA, Brasília.

Baptista, V.B. da S., Córcoles, J.I., Colombo, A., Moreno, M.Á., 2019. Feasibility of the use of variable speed drives in center pivot systems installed in plots with variable topography. Water (Switzerland) 11, 2192. https://doi.org/10.3390/w11102192.

Batista, P.V.G., Davies, J., Silva, M.L.N., Quinton, J.N., 2019. On the evaluation of soil erosion models: are we doing enough ? Earth Sci. Rev. 197, 102898. https://doi.org/10.1016/j.earscirev.2019.102898.

Batista, P.V.G., Baptista, V.B. da S., Wilken, F., Seufferheld, K., Quinton, J.N., Fiener, P., 2023a. Erosion-classification data for centre-pivot-irrigated fields in Cristalina, Brazil. Zenodo. https://doi.org/10.5281/zenodo.7680625 (dataset).

Batista, P.V.G., Evans, D.L., Cândido, B.M., Fiener, P., 2023b. Does soil thinning change soil erodibility? An exploration of long-term erosion feedback systems. SOIL 9, 71–88. https://doi.org/10.5194/soil-9-71-2023.

Bennett, N.D., Croke, B.F.W., Guariso, G., Guillaume, J.H.a., Hamilton, S.H., Jakeman, A.J., Marsili-Libelli, S., Newham, L.T.H., Norton, J.P., Perrin, C., Pierce, S.A., Robson, B., Seppelt, R., Voinov, A.A., Fath, B.D., Andreassian, V., 2013. Characterising performance of environmental models. Environ. Model. Softw. 40, 1–20. https://doi.org/10.1016/j.envsoft.2012.09.011.

Bjorneberg, D.L., Ippolito, J.A., King, B.A., Nouwakpo, S.K., Koehn, A.C., 2020. Moving toward sustainable irrigation in a southern Idaho irrigation project. Trans. ASABE 63, 1441–1449. https://doi.org/10.13031/TRANS.13955.

Boardman, J., 2016. The value of Google Earth TM for erosion mapping. Catena 143, 123–127. https://doi.org/10.1016/j.catena.2016.03.031.

Boardman, J., Evans, R., 2020. The measurement, estimation and monitoring of soil erosion by runoff at the field scale: challenges and possibilities with particular reference to Britain. Prog. Phys. Geogr. 44, 31–49. https://doi.org/10.1177/0309133319861833.

Castillo, C., Pérez, R., James, M.R., Quinton, J.N., Taguas, E.V., Gómez, J.A., 2012. Comparing the accuracy of several field methods for measuring gully erosion. Soil Sci. Soc. Am. J. 76, 1319. https://doi.org/10.2136/sssaj2011.0390.

Cerdan, O., Le Bissonnais, Y., Couturier, A., Bourennane, H., Souchère, V., 2002. Rill erosion on cultivated hillslopes during two extreme rainfall events in Normandy, France. Soil Tillage Res. 67, 99–108. https://doi.org/10.1016/S0167-1987(02)00045-4.

Didoné, E.J., Minella, J.P.G., Evrard, O., 2017. Measuring and modelling soil erosion and sediment yields in a large cultivated catchment under no-till of Southern Brazil. Soil Tillage Res. 174, 24–33. https://doi.org/10.1016/j.still.2017.05.011.

Didoné, E.J., Minella, J.P.G., Tiecher, T., Zanella, R., Prestes, O.D., Evrard, O., 2021. Mobilization and transport of pesticides with runoff and suspended sediment during flooding events in an agricultural catchment of Southern Brazil. Environ. Sci. Pollut. Res. 28, 39370–39386. https://doi.org/10.1007/s11356-021-13303-z.

EMATER – Agência Goiana de Assitência Técnica, Extensão Rural e Pesquisa Agropecuária, 2016. Distribuição dos solos de Goiás (1:250 000). Accessed 31 Augst 2022. http://www.sieg.go.gov.br/siegdownloads/.

Fiener, P., Auerswald, K., 2003. Effectiveness of grassed waterways in reducing runoff and sediment delivery from agricultural watersheds. J. Environ. Qual. 32, 927–936. https://doi.org/10.2134/jeq2003.9270.

Fischer, F.K., Kistler, M., Brandhuber, R., Maier, H., Treisch, M., Auerswald, K., 2018. Validation of official erosion modelling based on high-resolution radar rain data by aerial photo erosion classification. Earth Surf. Process. Landf. 43, 187–194. https://doi.org/10.1002/esp.4216.

Garrett, R.D., Koh, I., Lambin, E.F., le Polain de Waroux, Y., Kastens, J.H., Brown, J.C., 2018. Intensification in agriculture-forest frontiers: land use responses to development and conservation policies in Brazil. Glob. Environ. Chang. 53, 233–243. https://doi.org/10.1016/j.gloenvcha.2018.09.011.

Gilley, J.R., 1984. Suitability of reduced pressure center-pivots. J. Irrig. Drain. Eng. 110, 22–34. https://doi.org/10.1061/(asce)0733-9437(1984)110:1(22).

Gulhati, N.D., Smith, W.C., 1967. Irrigated agriculture: an historical review. In: Hagan, R.M., Haise, H.R., Edminster, T.W. (Eds.), Irrigation of Agricultural Lands. American Society of Agronomy, Madison, pp. 3–11 https://doi.org/10.2134/agronmonogr11.c1.

Hasheminia, S.M., 1994. Controlling runoff under low pressure center pivot irrigation systems. Irrig. Drain. Syst. 8, 25–34. https://doi.org/10.1007/BF00880796.

Hörbe, T., Minella, J.P.G., Schneider, F.J.A., Londero, A.L., Gubiani, P.I., Merten, G.H., Schlesner, A., 2021. Managing runoff in rainfed agriculture under no-till system: potential for improving crop production. Rev. Bras. Cienc. do Solo 45, 1–17. https://doi.org/10.36783/18069657rbcs20210015.

Hunke, P., Mueller, E.N., Schröder, B., Zeilhofer, P., 2015. The Brazilian Cerrado: assessment of water and soil degradation in catchments under intensive agricultural use. Ecohydrology 8, 1154–1180. https://doi.org/10.1002/eco.1573.

IBGE – Insituto Brasileiro de Geografia e Estatística, 2017. Censo agropecuário de 2017. Accessed 26 November 2022. https://cidades.ibge.gov.br/brasil/go/cristalina/pesquisa/24/27745.

Ippolito, J.A., Bjorneberg, D., Stott, D., Karlen, D., 2017. Soil quality improvement through conversion to sprinkler irrigation. Soil Sci. Soc. Am. J. 81, 1505–1516. https://doi.org/10.2136/sssaj2017.03.0082.

Johansen, K., Lopez, O., Tu, Y.H., Li, T., McCabe, M.F., 2021. Center pivot field delineation and mapping: a satellite-driven object-based image analysis approach for national scale accounting. ISPRS J. Photogramm. Remote Sens. 175, 1–19. https://doi.org/10.1016/j.isprsjprs.2021.02.019.

Kincaid, D.C., 2002. The WEPP model for runoff and erosion prediction under sprinkler irrigation. Trans. ASAE 45, 67–72. https://doi.org/10.13031/2013.7875.

Kincaid, D.C., 2005. Application rates from center pivot irrigation with current sprinkler types. Appl. Eng. Agric. 21, 605–610.

Kincaid, D.C., McCann, I., Bush, J.R., Hasheminia, M., 1990. Low pressure center pivot irrigation and reservoir tillage. Visions of the Future, Proceendings of the Third National Irrigation Symposyum. American Society of Agricultural Engineers, pp. 54–60.

King, B.A., 2016. Moving spray-plate center-pivot sprinkler rating index for assessing runoff potential. Trans. ASABE 59, 225–237. https://doi.org/10.13031/trans.59.11162.

King, B.A., Bjorneberg, D.L., 2011. Evaluation of potential runoff and erosion of four center pivot irrigation sprinklers. Appl. Eng. Agric. 27, 75–85. https://doi.org/10.13031/2013.36226.

Lehrsch, G.A., Lentz, R.D., Bjorneberg, D.L., Sojka, R.E., 2014. Irrigation-Induced, Reference Module in Earth Systems and Environmental Sciences. Elsevier Inc. https://doi.org/10.1016/b978-0-12-409548-9.09019-9.

Lian, J., Li, Yulin, Li, Yuqiang, Zhao, X., Zhang, T., Wang, Xinyuan, Wang, Xuyang, Wang, L., Zhang, R., 2022. Effect of center-pivot irrigation intensity on groundwater level dynamics in the agro-pastoral ecotone of northern China. Front. Environ. Sci. 10, 1–12. https://doi.org/10.3389/fenvs.2022.892577.

Londero, A.L., Minella, J.P.G., Schneider, F.J.A., Deuschle, D., Merten, G.H., Evrard, O., Boeni, M., 2021. Quantifying the impact of no-till on sediment yield in southern Brazil at the hillslope and catchment scales. Hydrol. Process. 35, 1–16. https://doi.org/10.1002/hyp.14286.

Lopes, A.S., Guilherme, L.R.G., 2016. A Career Perspective on Soil Management in the Cerrado Region of Brazil, Advances in Agronomy. Elsevier Inc. https://doi.org/10.1016/bs.agron.2015.12.004.

Marques, J.J., Schulze, D.G., Curi, N., Mertzman, S.A., 2004. Major element geochemistry and geomorphic relationships in Brazilian Cerrado soils. Geoderma 119, 179–195. https://doi.org/10.1016/S0016-7061(03)00260-X.

Martin, D., Kranz, W.L., Smith, T., Irmak, S., Burr, C., Yoder, R., 2017. Center Pivot Irrigation Handbook. University of Nebraska-Lincoln, Lincoln.

Nakawuka, P., Okwany, R.O., Peters, R.T., Desta, K., Sadeghi, S.H., 2014. Efficacy of boom systems in controlling runoff under center pivots and linear move irrigation systems. Appl. Eng. Agric. 30, 797–801. https://doi.org/10.13031/aea.30.10540.

Panachuki, E., Bertol, I., Sobrinho, T.A., de Oliveira, P.T.S., Rodrigues, D.B.B., 2011. Soil and water loss and water infiltration in red latosol under different management systems. Rev. Bras. Cienc. do Solo 35, 1777–1785. https://doi.org/10.1590/s0100-06832011000500032.

Phocaides, A., 2000. Technical Handbook on Pressurized Irrigation Techniques. FAO, Rome.

Prasuhn, V., 2020. Twenty years of soil erosion on-farm measurement: annual variation, spatial distribution and the impact of conservation programmes for soil loss rates in Switzerland. Earth Surf. Process. Landf. 45, 1539–1554. https://doi.org/10.1002/esp.4829.

Puy, A., Lo Piano, S., Saltelli, A., 2020. Current models underestimate future irrigated areas. Geophys. Res. Lett. 47, 1–10. https://doi.org/10.1029/2020GL087360.

Quinton, J.N., Catt, J.A., 2007. Enrichment of heavy metals in sediment resulting from soil erosion on agricultural fields. Environ. Sci. Technol. 41, 3495–3500. https://doi.org/10.1021/es062147h.

Quinton, J.N., Öttl, L.K., Fiener, P., 2022. Tillage exacerbates the vulnerability of cereal crops to drought. Nat. Food 3, 472–479. https://doi.org/10.1038/s43016-022-00533-8.

R Core Team, 2023. R: A Language for Statistical Computing. R Foundation for Statistical Computing, Vienna, Austria. https://www.R-project.org/.

Rosa, L., 2022. Adapting agriculture to climate change via sustainable irrigation: biophysical potentials and feedbacks. Environ. Res. Lett. 17, 063008. https://doi.org/10.1088/1748-9326/ac7408.

Saggau, P., Kuhwald, M., Hamer, W.B., Duttmann, R., 2022. Are compacted tramlines underestimated features in soil erosion modeling? A catchment-scale analysis using a process-based soil erosion model. L. Degrad. Dev. 33, 452–469. https://doi.org/10.1002/ldr.4161.

Siebert, S., Kummu, M., Porkka, M., Döll, P., Ramankutty, N., Scanlon, B.R., 2015. A global data set of the extent of irrigated land from 1900 to 2005. Hydrol. Earth Syst. Sci. 19, 1521–1545. https://doi.org/10.5194/hess-19-1521-2015.

Silgram, M., Jackson, D.R., Bailey, A., Quinton, J., Stevens, C., 2010. Hillslope scale surface runoff, sediment and nutrient losses associated with tramline wheelings. Earth Surf. Process. Landf. 35, 699–706. https://doi.org/10.1002/esp.1894.

Silva, L.L., 2006. The effect of spray head sprinklers with different deflector plates on irrigation uniformity, runoff and sediment yield in a Mediterranean soil. Agric. Water Manag. 85, 243–252. https://doi.org/10.1016/j.agwat.2006.05.006.

Silva, L.L., 2017. Are basin and reservoir tillage effective techniques to reduce runoff under sprinkler irrigation in Mediterranean conditions? Agric. Water Manag. 191, 50–56. https://doi.org/10.1016/j.agwat.2017.06.003.

Van Oost, K., Govers, G., Cerdan, O., Thauré, D., Van Rompaey, a., Steegen, a., Nachtergaele, J., Takken, I., Poesen, J., 2005. Spatially distributed data for erosion model calibration and validation: the Ganspoel and Kinderveld datasets. Catena 61, 105–121. https://doi.org/10.1016/j.catena.2005.03.001.

Wang, X., Müller, C., Elliot, J., Mueller, N.D., Ciais, P., Jägermeyr, J., Gerber, J., Dumas, P., Wang, C., Yang, H., Li, L., Deryng, D., Folberth, C., Liu, W., Makowski, D., Olin, S., Pugh, T.A.M., Reddy, A., Schmid, E., Jeong, S., Zhou, F., Piao, S., 2021. Global irrigation contribution to wheat and maize yield. Nat. Commun. 12, 1–8. https://doi.org/10.1038/s41467-021-21498-5.

Zweifel, L., Meusburger, K., Alewell, C., 2019. Spatio-temporal pattern of soil degradation in a Swiss Alpine grassland catchment. Remote Sens. Environ. 235, 111441. https://doi.org/10.1016/j.rse.2019.111441.